

Проведені теоретичні дослідження електромагнітних процесів в активній частині якоря електричної машини в динамічному режимі короткого замикання за допомогою трьохмірної моделі магнітного поля, представленій у вигляді сполучення електричних кіл фазових обмоток і геометричних 3D областей. Запропоновано підхід щодо визначення власних та взаємних індуктивностей між фазними обмотками якоря електричних машин, оснований на декомпозиції електромагнітних процесів, шляхом комбінацій вмикання фазних обмоток якоря до мережі. Визначені закономірності електромагнітних процесів від власних і взаємних впливів фазних струмів якоря, які викликають появу ефектів само- й взаємної індукції з та без врахування магнітних властивостей матеріалів. Розглянуті явища самоіндукції у фазах обмотки якоря, створення складових індуктивних струмів у фазі від дії фазних струмів сусідніх фаз, а також їхніх підмагнічуючих і розмагнічуючих властивостей. Вплив цих процесів призводить до несиметрії систем взаємних індуктивностей між фазами обмотки, однак при цьому не порушується симетрія повних індуктивностей фазних обмоток якоря. Для більш точного визначення індуктивних параметрів обмотки якоря електричної машини за класичною методикою запропоновані відповідні коефіцієнти корекції. Це дозволить мінімізувати струмові похибки і забезпечити адекватність загальновідомих трьох- і двофазних моделей електричних машин, заснованих на системах диференціальних рівнянь першого порядку. Достовірність і точність отриманих даних 3D моделювання магнітних полів підтверджується результатами фізичних випробувань. При врахуванні магнітних властивостей електрофізичних матеріалів активної частини якоря електричної машини відносна струмова похибка не перевищує  $2,68 \pm 2,91$  %, без урахування магнітних властивостей –  $103,09 \pm 106,32$  %

**Ключові слова:** електрична машина, електромагнітне поле, індуктивні параметри, трьохмірна польова модель

Received date 29.08.2019

Accepted date 20.11.2019

Published date 21.12.2019

## 1. Introduction

Further improvement of designs and development of the theory of electrical machines (EM) are directly related to the search for new technical solutions and technologies. This would ensure creation of devices with improved technical characteristics and high indicators of power efficiency of regulated electric drives, autonomous power supply systems for a series of consumers in industry, power engineering, agriculture and special-purpose devices.

The most common types of electric machines are asynchronous and synchronous [1, 2], synchronous with permanent magnets [3, 4], and synchronous with combined stator windings [5]. They have a fundamentally similar core design

and a system of three-phase armature winding the main task of which is formation of rotating magnetic field. Uniform distribution of rotating magnetic field and installed power of the EM armature, starting current and maximum torque depend on the ratio of active and inductive resistances (dissipative and mutual inductances) of phase windings [1]. Well-known engineering procedures take into account design features of phase windings and active part of the EM stator just approximately and do not enable determination of its parameters with high accuracy. Therefore, error in design calculations of the winding data and active part of the EM stator is at least 15 %.

In this regard, many issues related to the processes of electromagnetic and electromechanical conversion of energy including features of determining inductive parameters of

UDC 621.313.3

DOI: 10.15587/1729-4061.2019.185136

# IMPROVING EFFICIENCY IN DETERMINING THE INDUCTANCE FOR THE ACTIVE PART OF AN ELECTRIC MACHINE'S ARMATURE BY METHODS OF FIELD MODELING

**M. Kotsur**

PhD, Associate Professor  
Department of Electrical and  
Electronic Apparatuses\*\*  
E-mail: kotsur8@gmail.com

**D. Yarymbash**

Doctor of Technical Sciences, Associate Professor\*  
E-mail: yarymbash@gmail.com

**I. Kotsur**

PhD, Associate Professor\*  
E-mail: igor.m.kotsur@gmail.com

**S. Yarymbash**

PhD, Associate Professor\*  
E-mail: kstj06@gmail.com

\*Department of Electrical Machines\*\*

\*\*Zaporizhzhia Polytechnic National University  
Zhukovskoho str., 64, Zaporizhzhia, Ukraine, 69063

Copyright © 2019, M. Kotsur, D. Yarymbash, I. Kotsur, S. Yarymbash

This is an open access article under the CC BY license

(<http://creativecommons.org/licenses/by/4.0>)

EM armature have not been studied sufficiently [6]. This would make it possible to take more accurately into account magnetic coupling with various electrotechnical complexes and power systems and their mutual influence on features of their work. This determines relevance of high-precision and highly efficient methods for calculating inductive parameters of phase windings of EM armature at the stages of their design and modernization.

## 2. Literature review and problem statement

It is known that classical methods applied in calculation of parameters [1] and characteristics [2] of EMs and analysis of their operation in various modes are based on a series of assumptions [6]. They lead to an essential calculation error and cannot be used for optimization [7] and design [8] of modern energy-efficient electric drive systems. Along with classical methods, methods for calculating parameters and characteristics of transformers [9], EM [10] and converters [11] are the most popular today in engineering practice as well as among researchers. They are based on the theory of electric and magnetic circuits. Depending on operating modes of electrotechnical and electromechanical systems, these calculation methods are grounded on commonly known exchange circuits and are built on a series of assumptions and simplifications. Moreover, authors do not take into account influence of surface effects [12], multicomponent spatial structure [13], nonlinear electrophysical [14] and magnetic [15] properties of active materials and winding circuits [16]. All these assumptions cause a decrease in accuracy of determining active and inductive parameters of phase windings of the EM armature.

A more complete account of influence of design features of active part of the EM armature on parameters of their phase windings as well as nonlinear properties of structural materials was made by authors of [17] using field modeling and parametric analysis [18]. However, in multicomponent sections of the active part with nonlinear electrophysical properties, computer implementation of a model based on finite element methods is complicated by large time consumption and requirements to computing resources [19]. A three-dimensional model of electromagnetic processes was proposed in [20] for determining electrical parameters. However, its use is limited and possible only for the systems with materials having linear magnetic properties. For effective numerical implementation of field models for EM [21] and transformers [22], it was proposed to use differentiation of sizes of finite elements and approximations by first-order Lagrange polynomials. Application of this approach would significantly reduce computation and time resources when modeling in a PC. Some authors try to simplify geometric model [23], refine nonlinearity of electrophysical and magnetic [24] properties by empirical dependences or use two-dimensional models [25]. These assumptions and simplifications reduce accuracy of modeling results. To obtain high-precision calculation results, the model of electromagnetic field of armature and the EM in general must reflect in detail multicomponent structure of the active part and take into account nonlinearity of electrophysical and magnetic properties of active materials. Effectiveness of numerical implementation of the three-dimensional EM model must correspond to requirements of the problems of design parameter optimization. This necessitates development of special approaches that will improve accuracy and efficiency of calculations and ensure ad-

aptation of three-dimensional field modeling to the problems of optimal design and calculation of EM parameters.

## 3. The aim and objectives of the study

The study objective consists in development of an effective approach to determining self- and mutual inductances of phase armature windings by the method of circuit-field modeling taking into account magnetic and electrophysical properties and design features of multicomponent EM elements.

To achieve this objective, the following tasks were set:

- elaborate mathematical description of a circuit-field 3D model of electromagnetic field reflecting features of electromagnetic energy conversion taking into account magnetic properties of materials for active part of the EM armature with multicomponent design elements;
- establish laws of dependence of electromagnetic processes on self- and mutual influences of phase currents of the armature causing appearance of effects of self- and mutual induction in presence and absence of magnetic properties of materials of the active part of the EM armature;
- determine self- and mutual inductances of dissipation from phase windings in presence and absence of magnetic properties of materials of active part of the EM armature and correction coefficients for inductive parameters of the EM armature phase windings calculated by a classical engineering procedure in order to minimize current errors.

## 4. Development and mathematical description of a circuit-field 3D model of electromagnetic processes in the electric machine armature

A 3D calculation range of field modeling of electromagnetic processes occurring in the active part of the tested synchronous machine (SM) armature includes the following subranges: armature core 1; three-phase armature winding 2; insulation system 3 in the groove zone of the armature core. A coil group of the armature winding consists of frontal and groove parts which are geometrically connected and form an solid coil group. Coil groups are geometrically symmetrical. Each coil group of the winding has input 4 and output 5 (Fig. 1).

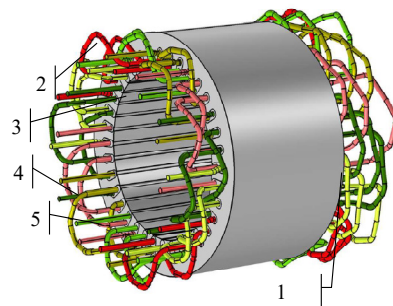


Fig. 1. Geometric model of the active part of armature of the tested synchronous machine: armature core 1; three-phase armature winding 2; insulation system 3 in the groove zone of the armature core; inputs 4 and outputs 5 of coil groups of the armature winding

In mathematical description of electromagnetic processes, assumptions of isotropy of electrophysical and electro-

magnetic properties of materials, absence of bias currents and free charges are made [26]. In this case, non-stationary electromagnetic processes in the SM in a short-circuit mode can be described by a conjugated system of nonlinear partial differential equations [27]:

$$\begin{cases} \sigma_j \partial A_j / \partial \tau + \sigma_j (\theta_j) \nabla V_j + \\ + \nabla \times \left[ (\mu_0 \mu_j(B))^{-1} \nabla \times A_j \right] = J_{ej}; \\ -\nabla \cdot \partial (\varepsilon_0 \varepsilon_r \nabla V_j) / \partial \tau - \\ -\nabla \cdot (\sigma_j (\theta_j) \cdot \nabla V_j - J_{ej}) = 0, \end{cases} \quad (1)$$

where  $A$  is vector magnetic potential;  $V$  is electric potential;  $\sigma(\Theta)$  is electrical conductivity;  $B$  is magnetic field induction;  $\mu$  is relative magnetic permeability;  $\varepsilon_r$  is relative dielectric constant;  $\Theta$  is temperature;  $\omega$  is angular frequency;  $J_e$  is density of external current source;  $j$  indices correspond to subranges of geometric calculation range (Fig. 1).

In accordance with [28], the equation system (1) is supplemented with the Coulomb calibration condition  $\text{div}(A)=0$ .

The conditions of conjugation for magnetic and electric fields can be formulated as in [30]:

$$\begin{cases} n_{i,k} \times (H_i - H_k) = 0 \Big|_{\forall i,k \in (1,6), i \neq k}, \\ H = (\mu_0 \mu)^{-1} \nabla \times A, \\ n_{i,k} \cdot (J_i - J_k) = 0 \Big|_{\forall i,k \in (1,6), i \neq k}, \\ J = \sigma(\theta) \cdot E, \quad E = -\nabla V - j\omega A, \end{cases} \quad (2)$$

where  $H$  is the magnetic field strength;  $E$  is the electric field strength.

Boundary conditions are set at external boundaries of the computation range [30]:

$$\begin{cases} A_j = 0 \Big|_{\forall j \in (1,6)}, \quad A_j = \bar{k} \cdot A_y(x, z) \Big|_{j=1}, \\ V_j = \phi_j \Big|_{\forall j \in (2,6)}, \\ n_j \cdot (J_j) = 0 \Big|_{j=1}. \end{cases} \quad (3)$$

Temperature conditions of the SM are considered stationary and estimated in accordance with [31].

Design of a two-layer winding of the SM armature contains four coil groups with three coils in each coil group per phase. The first and third, second and fourth coil groups are interconnected in series. The second and fourth coil groups are connected in parallel to the first and third coil groups. Outputs of coil groups of all phases are Y-system connected (Fig. 2).

Initial conditions correspond to the first law of switching:

$$\begin{cases} i_A|_{0-} = i_A|_{0+} = 0; \\ i_B|_{0-} = i_B|_{0+} = 0; \\ i_C|_{0-} = i_C|_{0+} = 0; \\ u_A|_{0+} = 0; \\ u_B|_{0+} = \sqrt{2}U_{fase} \sin(2\pi/3); \\ u_C|_{0+} = \sqrt{2}U_{fase} \sin(4\pi/3). \end{cases} \quad (4)$$

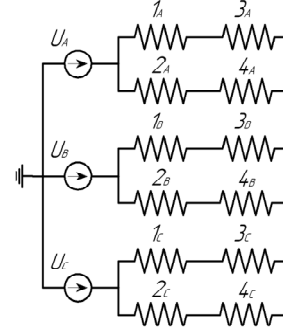


Fig. 2. Electric circuit of model implementation of power supply of coil groups of the synchronous machine armature phase windings

Geometric model of the armature winding coil in the tested SM (Fig. 2) is implemented as a single turn consisting of one effective conductor. To take into account the number of turns, coil zones of the SM armature winding are described by the equation from [30]:

$$J_e = \frac{n \cdot I_{cir}}{A} e_{coil}, \quad (5)$$

where  $n$  is the number of turns in the winding;  $I_{cir}$  is a phase current;  $A$  is the cross section of an effective conductor;  $e_{coil}$  is the vector variable representing local density of effective conductors in a coil, length and cross section.

According to [32, 33], electrophysical processes in dielectric materials can be considered similar to the processes of electrical conductivity in materials with a relatively small value of electrical conductivity.

For  $j$ -elements of the active part of the SM armature, magnetic field energy, its average values for each  $j$ -th zone, active losses of the armature windings and current density are calculated [22]:

$$\begin{cases} W|_j = \frac{1}{2} \iiint_{V_j} (\dot{B} \cdot \dot{H}) dx dy dz, \\ w|_j = W|_j / V_j; \quad V_j = \iiint_{V_j} dx dy dz, \\ P|_j = \iiint_{V_j} \sigma_j^{-1} J \cdot (J)^* dx dy dz, \\ J_j = -\sigma \cdot (\text{grad}(V_j) + j\omega A_j). \end{cases} \quad (6)$$

In addition, phase currents in the armature winding are calculated according to (5).

Computer implementation of the 3D field model (1)–(5) is performed in the structure of COMSOL Multiphysics software tools [28, 29]. Calculation subranges of the 3D model are divided into three-dimensional finite elements and have a tetrahedral shape. The tetrahedra faces are approximated by the first-order Lagrange polynomials which, according to [21], is sufficient to ensure high accuracy of calculations.

To improve efficiency of numerical implementation of the model, dimensions of finite 3D elements are differentiated. For the subregion of the anchor core made of cold rolled isotropic electrical steel with a pronounced nonlinearity of magnetic properties, dimensions of finite elements decrease and increase as they approach the outer boundary of the

calculation subrange. This makes it possible to implement numerically the model with high accuracy at smaller computational and time resources [21, 22].

**5. Studying the electromagnetic processes occurring in the active part of the synchronous machine armature**

**5. 1. Results obtained in the study of magnetic field in the active part of the armature of a synchronous machine**

Field 3D modeling of the electromagnetic field in the time-dependent statement of the problem in subregions of the active armature part was carried out on a sample of experimental SM. The experimental SM was built on the basis of a 2.6 kW MTF-111 induction motor with a non-factory four-pole two-layer armature winding. Design and diagram of connection of coil groups and phase windings of the armature fully complied with Fig. 1, 2. Inputs of the first and second coil groups of the three-phase winding were connected to an AC voltage source of 50 Hz industrial frequency. Angle of interphase shift was 120 el. grades. Phase voltage was corresponding to short-circuit voltage of  $0.5 U_{nom}$ .

Results of 3D modeling are presented by distribution of the z-component of magnetic potential vector  $A_z$  along entire active part of the armature (Fig. 3, a) and as XY-planes in the zones of  $S$  (plane 1) and  $j$  (plane 2) of the armature core length and in the zone of its face part (plane 3) (Fig. 3, b).

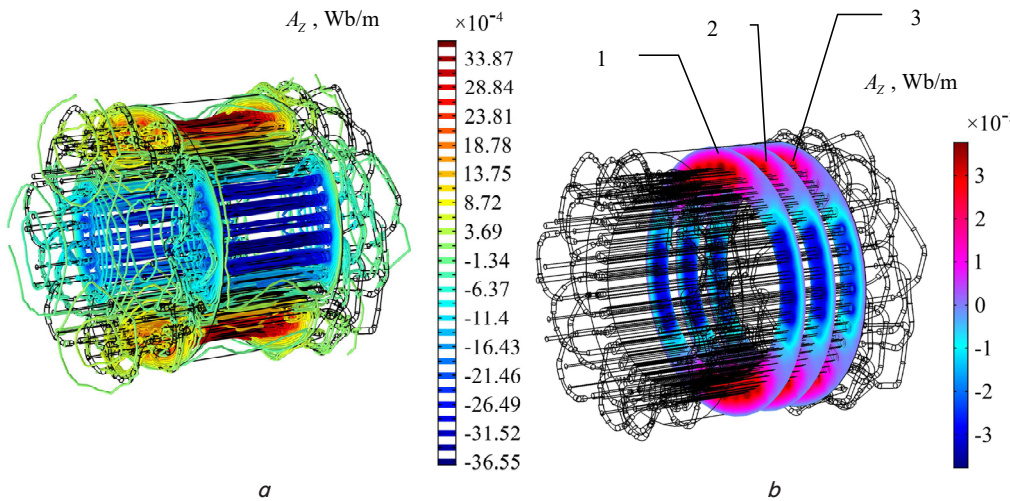


Fig. 3. Magnetic field in active part of the SM armature: a – Z-component of magnetic potential vector along entire active part; b – projection of magnetic potential vector onto XY axis of the active armature part

According to the data obtained from 3D field modeling, it was found that when testing the active part of the SM armature in a short-circuit (SC) mode, magnetic field is localized in the system of its phase windings. Surfaces of magnetic field localization close around bores of the armature core grooves and extend along entire zone of the grooves. Concentration of magnetic field decreases in the region of the face part of the core and beyond it, in the region of frontal parts of the winding. Moreover, values of  $A_z$  and magnetic field energy  $W_j$  were no more than 12 % of their values in the central region of the active armature part (Fig. 3, a). Magnetic field had a plane-parallel character (projections 1, 2, Fig. 3, b) in the central zone of the active core part measuring

up to 75–80 % of its length. Prevailing effects of self-induction and mutual surface induction and a series of other end effects were observed closer to the core face zones and in the region of frontal parts of the armature winding [2]. They were caused by peculiarities of distribution of scattering fields depending on the change in spatial orientation of frontal parts of the SM armature phase windings.

In order to study the effect of self-induction and mutual induction on electromagnetic parameters of the armature phase windings, cases of individual turn-on of each  $A, B, C$  phase and a group turn-on of  $A-B, B-C$  and  $C-A$  phases of the armature winding were considered. This approach has made it possible to apply the principle of superposition to the electromagnetic fields according to the Bio-Savart law [34] for the calculation range of the active part of the SM armature.

**5. 2. Establishing the laws of electromagnetic processes caused by self- and mutual influences of phase currents in the synchronous machine armature**

According to the data of numerical modeling, oscillograms of phase currents were obtained for corresponding cases of alternating turn-ons of phase windings of the SM armature (Fig. 4). When  $A-B$  phase windings are turned on, self-induction EMF is induced in the  $A$  phase with its vector aligned in concert with the phase voltage vector. In this case, a resulting vector of the  $A$  phase current ( $\vec{I}_A^{AB}$ ) is formed by summation of the current vector at the phase  $A$  turned on ( $\vec{I}_A^A$ ) and the vector of the current induced in  $A$  phase as a result of action of the  $B$  phase current ( $\vec{I}_A^B$ ).

The induced current  $\vec{I}_A^B$  is purely reactive and is of inductive nature. It is confirmed by presence of a lagging angle of the phase of  $\vec{I}_A^{AB}$  vector relative to the phase of  $\vec{I}_A^A$  vector (Fig. 4, a). When  $A-C$  phase windings are turned on, self-induction EMF is generated in the  $A$  phase with its vector directed opposite to the

phase voltage vector. In this case, a resulting vector of the  $A$  phase current ( $\vec{I}_A^{AC}$ ) is formed due to the difference between the current vector with the  $A$  phase turned on ( $\vec{I}_A^A$ ) and the vector of the current induced in the  $A$  phase as a result of action of the phase  $C$  current ( $\vec{I}_A^C$ ). The induced current  $\vec{I}_A^C$  is purely reactive and is of capacitive nature. This is confirmed by presence of the leading angle of the  $\vec{I}_A^{AC}$  vector phase relative to the  $\vec{I}_A^A$  vector phase (Fig. 4, a). When all phase windings are turned on, resulting current  $\vec{I}_A^{ABC}$  vector is formed which can also be determined from the following expression:

$$\vec{I}_A^{ABC} = \vec{I}_A^{AB} + \vec{I}_A^{AC} - \vec{I}_A^A. \tag{7}$$

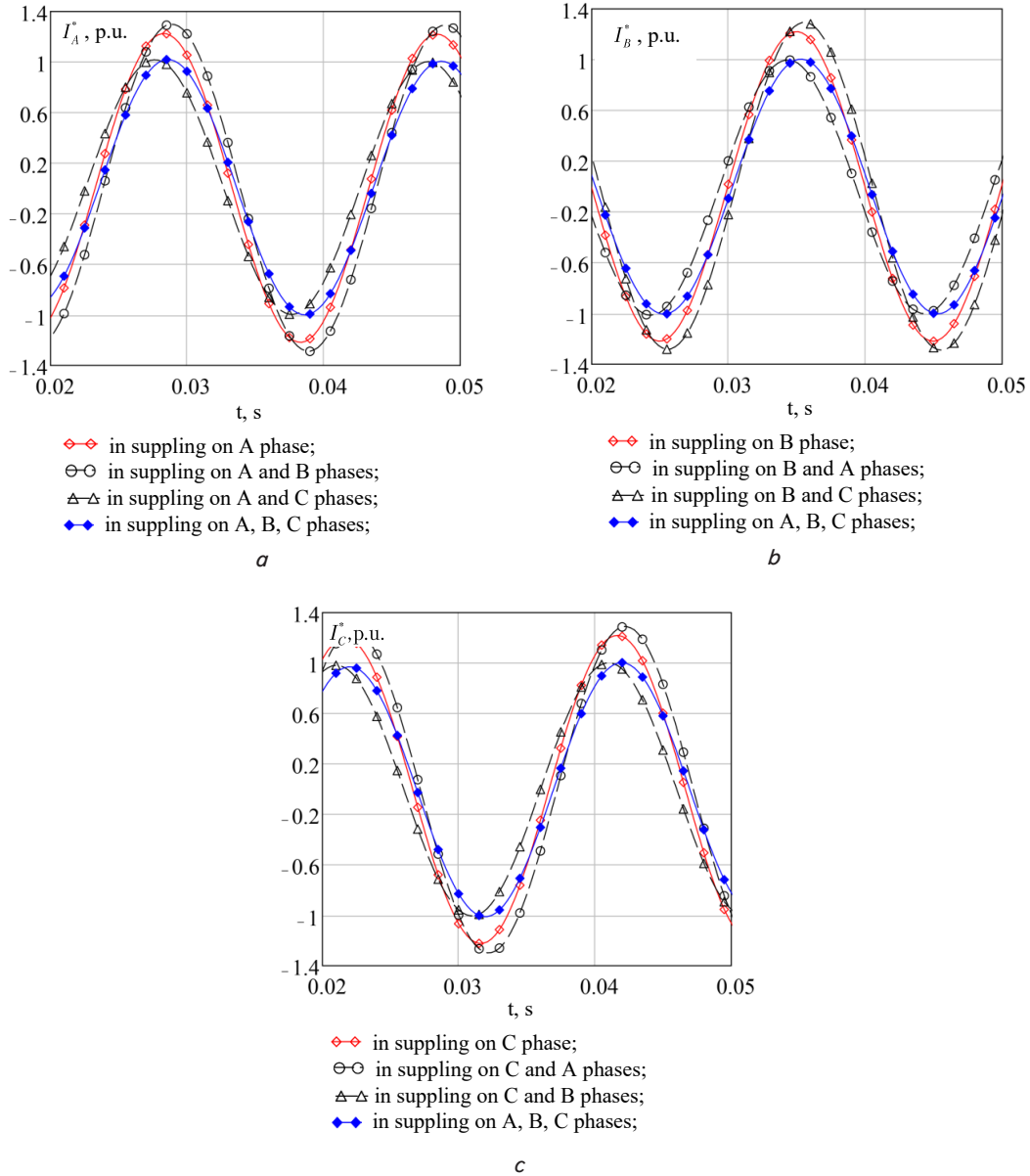


Fig. 4. Phase currents in various options of suppling on the phase windings of the SM armature: *a* – A phase; *b* – B phase; *c* – C phase

Expression (7) is also valid for determination of the resulting vectors of  $\vec{I}_B^{ABC}$  and  $\vec{I}_C^{ABC}$  current of other phases. Relative errors in calculation of resulting vectors of  $\vec{I}_A^{ABC}$ ,  $\vec{I}_B^{ABC}$  and  $\vec{I}_C^{ABC}$  phase currents obtained by numerical modeling and use of (7) with taking into account magnetic properties of the armature core ( $\mu = B(H)$ ) were  $\delta I_A^{ABC}|_{\mu=B(H)} = 0.851\%$ ,  $\delta I_B^{ABC}|_{\mu=B(H)} = 0.872\%$ ,  $\delta I_C^{ABC}|_{\mu=B(H)} = 0.839\%$ , respectively. If magnetic properties of the armature core are neglected ( $\mu = 1$ ), the figures are  $\delta I_A^{ABC}|_{(\mu=1)} = 2.65\%$ ,  $\delta I_B^{ABC}|_{(\mu=1)} = 2.662\%$ ,  $\delta I_C^{ABC}|_{(\mu=1)} = 2.541\%$ , respectively. According to expression (7), it is also possible to determine with sufficient accuracy any component of the phase current vectors. This will reduce the volume of tasks during modeling and total calculation time when determining parameters of the SM armature active part.

Fig. 5 shows components of induced phase currents  $\vec{I}_A^B$ ,  $\vec{I}_A^C$  for each phase of the winding with and without taking into account magnetic properties of the SM armature core. For the case when magnetic properties of the active armature part are not taken into account ( $\mu = 1$ ), demagnetizing effect of the C phase current promotes appearance of an induced component of  $\vec{I}_A^C$  current with a 1.15 times higher amplitude compared to the induced component of the  $\vec{I}_A^B$ , current resulting from magnetizing action of the neighboring B phase current. In this case, phase angle of  $\vec{I}_A^C$  vector is leading. The angle of phase shift between  $\vec{I}_A^C$  and  $\vec{I}_A^B$ , vectors is  $\phi_A^C - \phi_A^B = 240$  el. deg. In presence of magnetic properties of the SM armature active part (at  $\mu = B(H)$ ), amplitudes of vectors  $\vec{I}_A^B$  and  $\vec{I}_A^C$  were 2 times higher. In this case, the phase shift angle between  $\vec{I}_A^C$  and  $\vec{I}_A^B$  vectors increased by 1.2 times and amounted to  $\phi_A^C - \phi_A^B = 288$  el. deg. For B and C phases, there was similar manifestation of effects of mutual induction.

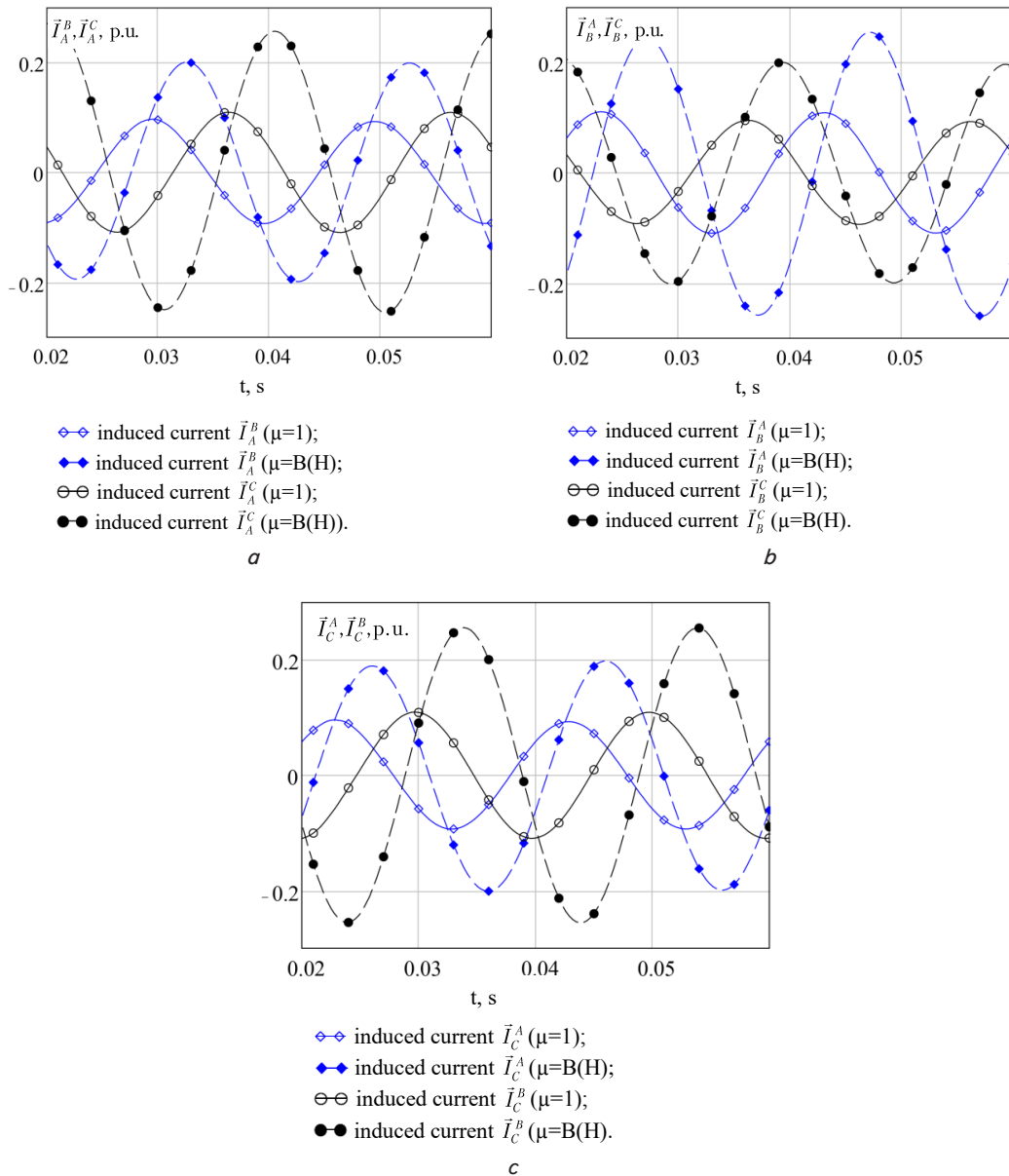


Fig. 5. Induced current components in phases of the armature winding: *a* – *A* phase; *b* – *B* phase; *c* – *C* phase

Thus, the induced components of  $\bar{I}_A^B$  and  $\bar{I}_B^A$  currents in the *A* and *B* phases formed by magnetizing current of the *B* phase and demagnetizing current of the *A* phase, respectively, form a mutual inductance between the *A* and *B* phases. In the case when  $\mu=1$ , values of mutual inductances will be the same due to equality of amplitudes of component currents  $\bar{I}_A^B$  and  $\bar{I}_B^A$ . In the case when  $\mu=B(H)$ , mutual inductances between these phases will be different because of absence of equality between amplitudes of the component currents  $\bar{I}_A^B$  and  $\bar{I}_B^A$ .

**5. 3. Determining self- and mutual inductances of armature phase windings of a synchronous machine**

In accordance with [22, 23] and based on the data obtained in calculating the values of magnetic field energy (6), self-dissipation inductances and mutual inductances between phases of the SM armature were determined:

$$L_{k,m} = \frac{2 \cdot W_{k,m}}{I_{k,m}^2}, \tag{8}$$

where *k, m* are corresponding indices of alternation of turning on phases of the ASM armature winding.

Total inductance of the armature winding phase can be determined from the following expression [2]:

$$\begin{cases} L_A = L_{AA} + M_{AB} + M_{AC}, \\ L_B = L_{BB} + M_{BA} + M_{BC}, \\ L_C = L_{CC} + M_{CA} + M_{CB}, \end{cases} \tag{9}$$

where *L, M* are dissipation inductances and mutual inductances between the *A, B* and *C* phases.

Proceeding from the data of numerical modeling and in accordance with (8), eigenvalues of dissipation inductances

and mutual inductances between the winding phases are given in Table 1. They were found with and without taking into account magnetic properties of the SM armature core. According to the EM theory [1, 2], mutual inductances of the armature phase windings were  $M_{AB}=M_{BA}=M_{AC}=M_{CA}=M_{BC}=M_{CB}=1/2 \cdot L_{AA}(L_{AA}=L_{BB}=L_{CC})$  which is confirmed by calculations according to (8) with  $\mu=1$  based on the modeling data with an error of  $\delta M|_{(\mu=1)} \leq 0,4 \%$ .

When magnetic properties of the active part of the SM armature were taken into account, only equality of self-dissipation inductances of the phase windings was preserved with values 3.5 higher than self-values at  $\mu=1$ . In presence of magnetizing and demagnetizing effects from currents of neighboring phases, symmetry of the mutual inductance system  $M_{AB} \neq M_{BA}; M_{AC} \neq M_{CA}; M_{BC} \neq M_{CB}$ . was violated. Despite this, symmetry of total inductances of the armature winding phases (9) was preserved, and according to the data in Table 1, it is  $L_A = 4.027 \cdot 10^{-3}$  H;  $L_B = 4.041 \cdot 10^{-3}$  H;  $L_C = 3.985 \cdot 10^{-3}$  H. Discrepancy error in terms of symmetry of total inductances of the armature winding phases was  $\delta L|_{(\mu=B(H))} = 0.224 \div 0.817 \%$ .

Table 1

Calculated values of dissipation inductance and mutual inductance between phases of the SM armature winding according to numerical modeling

Self-dissipation inductances of phase windings	With no taking into account magnetic properties ( $\mu=1$ )	With taking into account magnetic properties ( $\mu=B(H)$ )	Correction coefficients, $k_L$ , rel.un.
Self-dissipation inductances of phase windings, H			
$L_{AA}$	$0.914 \cdot 10^{-3}$	$3.256 \cdot 10^{-3}$	3.562
$L_{BB}$	$0.915 \cdot 10^{-3}$	$3.244 \cdot 10^{-3}$	3.545
$L_{CC}$	$0.918 \cdot 10^{-3}$	$3.264 \cdot 10^{-3}$	3.555
Mutual inductances between phase windings, H			
$M_{AB}$	$0.479 \cdot 10^{-3}$	$0.485 \cdot 10^{-3}$	1.02
$M_{AC}$	$0.423 \cdot 10^{-3}$	$0.286 \cdot 10^{-3}$	0.67
$M_{BA}$	$0.466 \cdot 10^{-3}$	$0.241 \cdot 10^{-3}$	0.52
$M_{BC}$	$0.428 \cdot 10^{-3}$	$0.556 \cdot 10^{-3}$	1.3
$M_{CA}$	$0.416 \cdot 10^{-3}$	$0.459 \cdot 10^{-3}$	1.1
$M_{CB}$	$0.436 \cdot 10^{-3}$	$0.262 \cdot 10^{-3}$	0.6

## 6. Discussion of the results obtained in modeling electromagnetic processes in the active armature part of the tested electric machine

Procedures of calculating inductive parameters of the SM armature winding based on classical EM theory are valid if magnetic properties ( $\mu=1$ ) of materials of the active part of the SM armature are not taken into account. This was confirmed by verification of inductive parameters according to the field modeling data (Table 2). Based on the results of field modeling, description of the phenomena of self-induction in phases of armature winding and formation of components of induced currents in a phase from action of phase currents in neighboring phases were obtained and their magnetizing and demagnetizing properties were considered. These processes cause asymmetry of mutual inductance systems between winding phases but do not violate symmetry of total inductances of the armature winding phases. Electromagnetic parameters and ohmic resistances of the armature winding of the tested SM were validated by comparing them with the results of prototype tests conducted in

accordance with GOST 11828-86 at a laboratory of Zaporizhzhia Polytechnic National University, Ukraine (Fig. 6).



Fig. 6. General view of prototype anchor assembly of a synchronous machine: a – front view; b – rear view

Electromagnetic parameters of the armature winding were measured using OWON XDS3202E oscilloscope. According to the results of numerical modeling and actual measurements of the experimental sample, error in ohmic resistance of the armature phase windings was  $\delta R = 0.00694 \%$ . Relative values of current errors for numerical modeling shown in Table 2 were found from the following expression [22]:

$$\delta I = \left[ \frac{|I_t - I_s|}{I_t} \right] \cdot 100 \%, \tag{10}$$

where  $I_t, I_s$  are the values of currents according to the test data and numerical modeling, respectively.

Measurements were carried out both for turning on individual phases of the armature winding, A-B, A-C, B-C phase groups and a three-phase turning on.

The proposed approach to determination of self- and mutual inductances between phases of the SM armature winding ensures reliability and accuracy of the data obtained in 3D modeling of magnetic fields. This approach is based on decomposition of electromagnetic processes through combinations of turning in phase windings of the armature to the network using a combination of electrical circuits of phase windings and geometric 3D region of the active part of the SM armature. To ensure adequacy of the widely used well-known three- and two-phase EM models based on the systems of differential equations of the first order [6, 10], the calculated inductive parameters of their windings should be refined using correction coefficients  $k_L$  (Table 2).

Table 2

Current errors in the results of numerical modeling with the data of physical SM tests

Variants of turning on the armature phase winding	Current errors $\delta I$ , %	
	at $\mu=1$	at $\mu=B(H)$
Suppling on A-B-C phase group	103.09÷106.32	2.68÷2.91
Suppling on A-B phase group	98.12÷98.3	2.14÷2.32
Suppling on A-C phase group	98.2÷98.41	2.19÷2.29
Suppling on B-C phase group	98.15÷98.36	2.26÷2.84
Individual turning on A, B, C phases	112.6÷113.83	2.9÷3.36

Correction coefficients obtained in field modeling can be applied to inductive parameters of the armature winding

of the tested SM and the armature winding of EM of other series with similar designs. For other designs and parameters of windings and the core of EM armature, coefficients  $k_L$  should be determined according to the proposed approach. In the future, the approach proposed in this paper will be extended to determination of self- and mutual inductances of the rotor winding as well as the main inductances between phases of the armature windings and the SM rotor.

The results of this work can be applied to the problems of optimal design and calculation of EM parameters and in determining optimal magnetic compatibility of EM with elements of the electrotechnical complex and power systems. This will improve energy efficiency indicators of these elements depending on features of their operation.

## 7. Conclusions

1. It was established that mathematical description of the 3D circuit-field model of magnetic field of the active part of the EM armature with multicomponent elements of its structure reflect features of electromagnetic energy conversion. Reliability and accuracy of the results obtained in numerical modeling as well as the results of calculation of inductive parameters of the SM armature winding were substantiated by validating the calculation data of numerical modeling and the results of physical tests on a prototype EM. When taking into account magnetic properties of materials of the active part of the SM armature, relative current error did not exceed 2.68–2.91 % and when magnetic properties were not taken into account, the error was 103.09–106.32 %.

2. The phenomena of self- and mutual induction in phases of the armature winding, formation of components of induced currents in the phase under the action of phase currents in neighboring phases as well as their magnetizing and demagnetizing properties were considered. It was established that currents with a leading phase possess magnetizing property in a three-phase system of currents of the EM armature winding with respect to the phase under consideration. In this case, an induced current is formed in this phase. It is purely reactive and has an inductive character. Currents with a lagging phase have demagnetizing property. In this case, an induced current is formed which

is purely reactive and has a capacitive character. In the case when magnetic properties of materials are not taken into account ( $\mu=1$ ), their modular values are respectively 0.1–0.15 of the current module of a separately turned in phase. The slight predominance of the capacitive component of the induced current module is due to the fact that concentration of magnetic field decreases in the region of frontal parts of the winding. At the same time, value of the magnetic potential vector and the magnetic field energy make up no more than 12 % of their values in the central region of the active part of the armature which is a consequence of action of end effects from frontal parts of the phase windings of the SM armature. When taking into account magnetic properties of materials ( $\mu=B(H)$ ), their module values get 2 times higher which brings about a significant non-symmetry in terms of the modulus of inductance- and capacitance-induced currents in the phase. These laws of electromagnetic processes are also valid for other phases.

3. It has been found that self-dissipation inductances of the SM armature phase windings without taking into account magnetic properties of materials ( $\mu=1$ ) were equal by their values ( $L_{AA}=L_{BB}=L_{CC}$ ) and mutual inductances  $M_{AB}=M_{BA}=M_{AC}=M_{CA}=M_{BC}=M_{CB}$  were equal to  $1/2 L_{AA}$ . Discrepancy in mutual inductances between winding phases was  $\delta M|_{(\mu=1)} \leq 0.4$  %. When magnetic properties of the active part of the SM armature are taken into account, only equality of self- inductances of dissipation of phase windings is preserved. They were 3.5 times higher than self- values at  $\mu=1$ . Under action of magnetizing and demagnetizing effects from currents of neighboring phases, symmetry of the mutual inductance system  $M_{AB} \neq M_{BA}$ ;  $M_{AC} \neq M_{CA}$ ;  $M_{BC} \neq M_{CB}$  is broken. Despite this, symmetry of the complete inductances of the phases of the SM armature winding is preserved. The discrepancy error in terms of symmetry of total inductances of the armature winding phases was  $\delta L|_{(\mu=B(H))} = 0.224 \pm 0.817$  %. For accurate determination of inductive parameters of the SM armature winding by a classical method, correction coefficients for values of dissipative inductances and mutual inductances of the armature phase windings were determined taking into account magnetic properties of materials of the active part of the SM armature. This will make it possible to minimize current errors and ensure adequacy of widely used well-known three- and two-phase EM models based on the systems of differential equations of the first order.

## References

1. Kopylov, I. P., Klokov, B. K., Morozkin, V. P. (2005). Proektirovanie elektricheskikh mashin. Moscow: Vysshaya shkola, 767.
2. Ivanov-Smolenskiy, A. V. (2006). Elektricheskie mashiny. Moscow: Izdatel'skiy dom MEI, 532.
3. Ledovskiy, A. N. (1985). Elektricheskie mashiny s vysokokoertsitivnymi postoyannymi magnitami. Moscow: Energoatomizdat, 168.
4. Grebenikov, V. V., Pryymak, M. V. (2009). Issledovanie vliyaniya konfiguratsii magnitnoy sistemy na momentnye harakteristiki elektrodvigatelye s postoyannymi magnitami. Elektrotehnika i elektroenergetika, 2, 57–60.
5. Lushchik, V. D., Ivanenko, V. S. (2011). Bahatopoliusni kaskadni synkhronni mashyny. Elektromekhanichni i enerhozberihaiuchi systemy, 2, 116–123.
6. Kopylov, I. P. (2001). Matematicheskoe modelirovanie elektricheskikh mashin. Moscow: Vysshaya shkola, 327.
7. Tolochko, O. I., Ryzhkov, A. M. (2018). Synthesis and analysis of modal control system for crane mechanism motion taking into account the work of lifting mechanism. Tekhnichna Elektrodynamika, 2018 (4), 131–134. doi: <https://doi.org/10.15407/teched2018.04.131>
8. Kotsur, M. I., Andrienko, P. D., Kotsur, I. M., Bliznyakov, O. V. (2017). Converter for frequency-current slip-power recovery scheme. Scientific Bulletin of National Mining University, 4, 49–54.
9. Tykhovod, S. M. (2014). Transients modeling in transformers on the basis of magnetoelectric equivalent circuits. Electrical Engineering and Power Engineering, 2, 59–68. doi: <https://doi.org/10.15588/1607-6761-2014-2-8>
10. Tolochko, O. I., Buhrovyi, A. A. (2016). Improving dynamic of the system based on permanent magnet synchronous motor using optimal control strategies. Tekhnichna Elektrodynamika, 2016 (5), 35–37. doi: <https://doi.org/10.15407/teched2016.05.035>

11. German-Galkin, S. G. (2008). *Matlab & Simulink. Proektirovanie mehatronnyh sistem na PK*. Sankt-Peterburg: KORONA-VEK, 368.
12. Yu, D., Huang, X., Wu, L., Fang, Y. (2019). Design and Analysis of Outer Rotor Permanent-Magnet Vernier Machines with Overhang Structure for In-Wheel Direct-Drive Application. *Energies*, 12 (7), 1238. doi: <https://doi.org/10.3390/en12071238>
13. Wardach, M., Paplicki, P., Palka, R. (2018). A Hybrid Excited Machine with Flux Barriers and Magnetic Bridges. *Energies*, 11 (3), 676. doi: <https://doi.org/10.3390/en11030676>
14. Han, G., Chen, H., Shi, X. (2017). Modelling, diagnosis, and tolerant control of phase-to-phase fault in switched reluctance machine. *IET Electric Power Applications*, 11 (9), 1527–1537. doi: <https://doi.org/10.1049/iet-epa.2017.0185>
15. Bezverkhnia, Yu. S. (2019). A voltage loss preliminary estimation in ac busbars. *Naukovyi Visnyk Natsionalnoho Hirnychoho Universytetu*, 4, 73–78. doi: <https://doi.org/10.29202/nvngu/2019-4/13>
16. Yarymbash, D., Yarymbash, S., Kylymnyk, I., Divchuk, T., Litvinov, D. (2017). Features of defining three-phase transformer no-load parameters by 3D modeling methods. 2017 International Conference on Modern Electrical and Energy Systems (MEES). doi: <https://doi.org/10.1109/mees.2017.8248870>
17. Paiva Jr, R. D., Silva, V. C., Nabeta, S. I., Chabu, I. E. (2017). Magnetic topology with axial flux concentration: a technique to improve permanent-magnet motor performance. *Journal of Microwaves, Optoelectronics and Electromagnetic Applications*, 16 (4), 881–899. doi: <https://doi.org/10.1590/2179-10742017v16i4957>
18. Meng, X., Wang, S., Qiu, J., Zhu, J. G., Guo, Y. (2010). Cogging torque reduction of Bldc motor using level set based topology optimization incorporating with triangular finite element. *International Journal of Applied Electromagnetics and Mechanics*, 33 (3-4), 1069–1076. doi: <https://doi.org/10.3233/jae-2010-1222>
19. Shkaruplyo, V., Skrupsky, S., Oliinyk, A., Kolpakova, T. (2017). Development of stratified approach to software defined networks simulation. *Eastern-European Journal of Enterprise Technologies*, 5 (9 (89)), 67–73. doi: <https://doi.org/10.15587/1729-4061.2017.110142>
20. Aden Diriyé, A., Amara, Y., Barakat, G., Hlioui, S., De la Barrière, O., Gabsi, M. (2016). Performance analysis of a radial flux PM machine using a hybrid analytical model and a MBG reluctance network model. *European Journal of Electrical Engineering*, 18 (1-2), 9–26. doi: <https://doi.org/10.3166/ejee.18.9-26>
21. Kotsur, M., Yarymbash, D., Yarymbash, S., Kotsur, I. (2017). A new approach of the induction motor parameters determination in short-circuit mode by 3D electromagnetic field simulation. 2017 IEEE International Young Scientists Forum on Applied Physics and Engineering (YSF). doi: <https://doi.org/10.1109/ysf.2017.8126620>
22. Yarymbash, D., Kotsur, M., Subbotin, S., Oliinyk, A. (2017). A new simulation approach of the electromagnetic fields in electrical machines. 2017 International Conference on Information and Digital Technologies (IDT). doi: <https://doi.org/10.1109/dt.2017.8024332>
23. Benhamida, M. A., Ennassiri, H., Amara, Y. (2018). Reluctance network lumped mechanical & thermal models for the modeling and predesign of concentrated flux synchronous machine. *Open Physics*, 16 (1), 692–705. doi: <https://doi.org/10.1515/phys-2018-0088>
24. Thul, A., Steentjes, S., Schauerte, B., Klimczyk, P., Denke, P., Hameyer, K. (2018). Rotating magnetizations in electrical machines: Measurements and modeling. *AIP Advances*, 8 (5), 056815. doi: <https://doi.org/10.1063/1.5007751>
25. Yazdani-Asrami, M., Gholamian, S. A., Mirimani, S. M., Adabi, J. (2018). Calculation of AC Magnetizing Loss of ReBCO Superconducting Tapes Subjected to Applied Distorted Magnetic Fields. *Journal of Superconductivity and Novel Magnetism*, 31 (12), 3875–3888. doi: <https://doi.org/10.1007/s10948-018-4695-7>
26. Yarymbash, D., Yarymbash, S., Kotsur, M., Divchuk, T. (2018). Analysis of inrush currents of the unloaded transformer using the circuitfield modelling methods. *Eastern-European Journal of Enterprise Technologies*, 3 (5 (93)), 6–11. doi: <https://doi.org/10.15587/1729-4061.2018.134248>
27. Yarymbash, D., Yarymbash, S., Kotsur, M., Divchuk, T. (2018). Enhancing the effectiveness of calculation of parameters for short circuit of threephase transformers using field simulation methods. *Eastern-European Journal of Enterprise Technologies*, 4 (5 (94)), 22–28. doi: <https://doi.org/10.15587/1729-4061.2018.140236>
28. Yarymbash, D., Kotsur, M., Bezverkhnia, Y., Yarymbash, S., Kotsur, I. (2018). Parameters Determination of the Trolley Busbars by Electromagnetic Field Simulation. 2018 IEEE 3rd International Conference on Intelligent Energy and Power Systems (IEPS). doi: <https://doi.org/10.1109/ieps.2018.8559576>
29. Yarymbash, D., Kotsur, M., Yarymbash, S., Kylymnyk, I. (2018). An Error Estimation Of The Current Sensors Of The Automated Control System Of The Technological Process Of Graphititation. 2018 IEEE 3rd International Conference on Intelligent Energy and Power Systems (IEPS). doi: <https://doi.org/10.1109/ieps.2018.8559489>
30. Yarymbash, D., Kotsur, M., Yarymbash, S., Divchuk, T. (2018). Electromagnetic Parameters Determination of Power Transformers. 2018 IEEE 3rd International Conference on Intelligent Energy and Power Systems (IEPS). doi: <https://doi.org/10.1109/ieps.2018.8559573>
31. Kotsur, M., Kotsur, I., Bezverkhnia, Y., Andrienko, D. (2017). Increasing of thermal reliability of a regulated induction motor in non-standard cycle time conditions. 2017 International Conference on Modern Electrical and Energy Systems (MEES). doi: <https://doi.org/10.1109/mees.2017.8248960>
32. Jacques, K., Steentjes, S., Henrotte, F., Geuzaine, C., Hameyer, K. (2018). Representation of microstructural features and magnetic anisotropy of electrical steels in an energy-based vector hysteresis model. *AIP Advances*, 8 (4), 047602. doi: <https://doi.org/10.1063/1.4994199>
33. Leuning, N., Steentjes, S., Stöcker, A., Kawalla, R., Wei, X., Dierdorf, J. et al. (2018). Impact of the interaction of material production and mechanical processing on the magnetic properties of non-oriented electrical steel. *AIP Advances*, 8 (4), 047601. doi: <https://doi.org/10.1063/1.4994143>
34. Stepanenko, A., Oliinyk, A., Deineha, L., Zaiko, T. (2018). Development of the method for decomposition of superpositions of unknown pulsed signals using the secondorder adaptive spectral analysis. *Eastern-European Journal of Enterprise Technologies*, 2 (9 (92)), 48–54. doi: <https://doi.org/10.15587/1729-4061.2018.126578>